Ethanol Modulates BK$_{Ca}$ Channels by Acting as an Adjuvant of Calcium[S]

Jianxi Liu[1], **Thirumalini Vaithianathan**[1], **Kandiah Manivannan**[3], **Abby Parrill**[2], and **Alejandro M. Dopico**[1]

[1] Department of Pharmacology, the University of Tennessee Health Science Center, Memphis, Tennessee

[2] Department of Chemistry, University of Memphis, Memphis, Tennessee

[3] Department of Physics, Astronomy, and Materials Science, Missouri State University, Springfield, Missouri

Abstract

Ethanol modulation of calcium- and voltage-gated potassium (slo1) channels alters neuronal excitability, cerebrovascular tone, brain function, and behavior, yet the mechanism of this modulation remains unknown. Using patch-clamp electrophysiology on recombinant BK$_{Ca}$ channels cloned from mouse brain and expressed in *Xenopus laevis* oocytes, we demonstrate that ethanol, even at concentrations maximally effective to modulate BK$_{Ca}$ channel function (100 mM), fails to gate the channel in absence of activating calcium. Moreover, ethanol does not modify intrinsic, voltage- or physiological magnesium-driven gating. The alcohol works as an adjuvant of calcium by selectively facilitating calcium-driven gating. This facilitation, however, renders differential ethanol effects on channel activity: potentiation at low (<10 μM) and inhibition at high (>10 μM) calcium, this dual pattern remaining largely unmodified by coexpression of brain slo1 channels with the neuronally abundant BK$_{Ca}$ channel β_4 subunit. Calcium recognition by either of the slo1 high-affinity sensors (calcium bowl and RCK1 Asp362/Asp367) is required for ethanol to amplify channel activation by calcium. The Asp362/Asp367 site, however, is necessary and sufficient to sustain ethanol inhibition. This inhibition also results from ethanol facilitation of calcium action; in this case, ethanol favors channel dwelling in a calcium-driven, low-activity mode. The agonist-adjuvant mechanism that we advance from the calcium-ethanol interaction on slo1 might be applicable to data of ethanol action on a wide variety of ligand-gated channels.

Large conductance calcium- and voltage-gated potassium (BK$_{Ca}$) channels, encoded by the *Slo1* (*KCNMA1*) gene are ubiquitous in the nervous system. Increases in channel activity in response to membrane depolarization and/or increase in internal calcium (Ca$_i^{2+}$) allow BK$_{Ca}$ channels to play an important role in action potential (AP) repolarization, after-hyperpolarizations that follow the AP or, in particular, trains of APs, and in controlling the release of neurotransmitters and neurohormones (Weiger et al., 2002; Salkoff et al., 2006).

Given the key role of BK$_{Ca}$ channels in controlling neuronal excitability and presynaptic secretion, it is not surprising that this channel type is functionally targeted by drugs that alter nervous system physiology and, thus, behavior. Indeed, several small amphiphiles, including local and general anesthetics and alcohols, have all been reported to modulate BK$_{Ca}$ channel

activity (Weiger et al., 2002). In particular, BK_{Ca} channel activity is increased by short-term exposure to ethanol concentrations obtained in circulation after alcohol consumption [i.e., ethanol <100 mM (Brodie et al., 2007)]. This ethanol action has been demonstrated to 1) accelerate AP repolarization in rat nucleus accumbens neurons (Martin et al., 2004), 2) decrease neuronal excitability in rat dorsal root ganglia, and thus is linked to alcohol-related analgesia (Gruss et al., 2001), and 3) inhibit the release of oxytocin and vasopressin from neurohypophysial nerve endings, the latter effect being linked to alcohol-induced diuresis (reviewed in Brodie et al., 2007). Finally, ethanol inhibition of cerebral artery BK_{Ca} channel activity contributes to alcohol-induced cerebrovascular constriction, a drug effect associated with moderate to heavy episodic drinking (Liu et al., 2004).

Ethanol modification of BK_{Ca} channel activity is modulated by a variety of factors, including post-translational modification of the channel-forming (slo1) subunit (Liu et al., 2006), coexpression of channel accessory subunits (Martin et al., 2004), and the lipid environment of the slo1 protein (Brodie et al., 2007). However, it is ethanol modification of slo1 channel gating that ultimately determines changes in BK_{Ca} activity and, thus, current (Dopico et al., 1998; Dopico, 2003; Martin et al., 2004). The central role of slo in alcohol actions in the body was underscored by demonstrating that BK_{Ca} channel activation in dopamine neurons is the major mechanism underlying ethanol-induced motor intoxication in *Caenorhabditis elegans*. In addition, mutations introduced to *Slo* by neuronal-specific promoters in *Drosophila melanogaster* prevent the acquisition of tolerance induced by ethanol (reviewed in Brodie et al., 2007). In synthesis, neuronal slo channel activity is modulated by ethanol, which contributes to major behavioral effects of the drug. Remarkably, the mechanisms and structural basis that determine ethanol modulation of slo1 channel gating, and thus activity, remain unknown.

Four basic processes define slo1 channel gating: intrinsic gating (channel constitutive activity), voltage-, Mg_i^{2+}-, and Ca_i^{2+}-driven gating (Cox and Aldrich, 2000). Moreover, gating by these biological signals is determined by distinct domains in the slo1 protein: the voltage sensor, the regulation of conductance for K^+ domain 1 (RCK1), which includes both a low-affinity Ca^{2+}/Mg^{2+} recognition site involved in gating by physiological Mg^{2+} and a high-affinity Ca^{2+}-recognition site, and the "calcium bowl" region. The latter and the RCK1 sense low Ca_i^{2+} over Mg_i^{2+} (Shi et al., 2002; Xia et al., 2002). Our study demonstrates that ethanol itself, at concentrations that modify slo1 currents and thus neuronal excitability and behavior, does not gate the slo1 channel or modify voltage-driven gating. Instead, ethanol requires physiological Ca_i^{2+}, but not Mg_i^{2+}, to alter channel activity. Ethanol is merely an adjuvant of activating Ca_i^{2+}, which leads to differential ethanol actions on BK_{Ca} P_o and thus current as a function of activating ligand. Finally, pinpoint mutagenesis results identified the channel structural domains that determine ethanol facilitation of Ca^{2+}-driven gating and the differential contribution of each domain to alcohol modulation of Ca^{2+} actions.

Materials and Methods

Mutagenesis and Expression

cDNAs coding for mouse brain slo1 (mslo; mbr5) inserted into the pBluescript vector were cut with ClaI and NotI and reinserted into the pBscMXT vector for expression in *Xenopus laevis* oocytes. Mslo mutants were constructed using QuikChange (Stratagene). Desired mutations and lack of unwanted mutations were confirmed by sequencing at the University of Tennessee Molecular Research Center. Mslo cDNAs were linearized with SalI and transcribed in vitro using T3 polymerase (Ambion, Austin, TX). BK_{Ca} β_4 cDNA inserted into the pOx vector was

linearized by NotI and transcribed using T3 polymerase. BK_{Ca} β_4 cDNA was a generous gift from Dr. Ligia Toro (UCLA).

Oocytes were removed and defolliculated as described previously (Dopico et al., 1998). Defolliculated oocytes were transferred to ND-96 solution (96 mM NaCl, 2 mM KCl, 1.8 mM $CaCl_2$, and 5 mM HEPES, pH 7.4, containing 2 mg/ml gentamicin and 2.5 mM Na^+ pyruvate). Mslo mbr5 cRNA was injected alone (0.1–1 ng/μl) or with BK_{Ca} β_4 (7.5 ng/μl) cRNA, giving molar ratios ≥6:1 (β:α). cRNA injection (23 nl/oocyte) was conducted using a modified micropipette (Drummond Scientific, Broomall, PA).

Electrophysiology Recordings

Immediately before recordings, oocytes were devitellinized as described previously (Dopico et al., 1998). Recordings were obtained from I/O patches 48 to 72 h after cRNA injection. The electrode solution contained 130 mM K^+ gluconate, 5.22 mM $CaCl_2$, 2.28 mM $MgCl_2$, 5 mM EGTA, 1.6 mM HEDTA, and 15 mM HEPES, pH 7.35, free Ca^{2+} = 11 ± 0.6 μM. Micromolar levels of external Ca^{2+} are widely known to improve Gigaseal formation and stability, while not modifying BK_{Ca} channel function (McManus, 1991; Priel et al., 2007). Bath solutions had varied composition, as follows. In the experiments in which the free Ca_i^{2+} was set to <1 μM, the solution contained 130 mM K^+ gluconate, 1 mM $MgCl_2$, 5 mM EGTA, and 15 mM HEPES, pH 7.35. In the experiments where the free Ca_i^{2+} was set to ≥1 μM, 1.6 mM HEDTA was added. In both cases, varying amounts of $CaCl_2$ (Dopico, 2003) were used to set the free Ca^{2+} at the desired level, keeping free Mg^{2+} constant at 1 mM. For the experiments conducted in zero Ca_i^{2+}, the bath solution contained 130 mM K^+ gluconate, 2.9 mM $MgCl_2$, 5 mM EGTA, 1.6 mM HEDTA, 15 mM HEPES, and 10 mM glucose, pH 7.35. For the experiments conducted in zero Mg_i^{2+}, the bath solution contained 130 mM K^+ gluconate, 5 mM EGTA, 1.6 mM HEDTA, 15 mM HEPES, 10 mM glucose, pH 7.35, with 5, 5.36, 6.1, 6.42, 6.63, and 6.88 mM $CaCl_2$ to achieve 1, 3, 10, 30, 100, and 300 μM free Ca^{2+}. In making the free Mg^{2+} solution having 0.3 μM free Ca^{2+}, HEDTA was omitted and 4.1 mM $CaCl_2$ was added. For the experiments with the combined 5D5N, D362A/D367A mutant at 1 mM free Ca_i^{2+}, the bath solution contained 130 mM K^+ gluconate, 7.5 mM $CaCl_2$, 1 mM $MgCl_2$, 5 mM EGTA, 1.6 mM HEDTA, 15 mM HEPES, pH 7.35. Free Ca^{2+} and Mg^{2+} were calculated using Max Chelator (Bers et al., 1994; http://www.stanford.edu/~cpatton/maxc.html) and experimentally validated using Ca^{2+}-sensitive/reference electrodes (Corning Life Sciences, Acton, MA) as described in detail somewhere else (Dopico, 2003).

Patch electrodes were pulled from glass capillaries (Drummond Scientific) as described previously (Dopico et al., 1998). The procedure gave tip resistances of 2 to 5 MΩ (for macropatch recordings) or 5 to 10 MΩ (for conventional I/O single-channel recordings) when filled with electrode solution. An Ag/AgCl electrode was used as ground electrode. After excision from the oocyte, the inner side of the membrane patch was exposed to bath solution containing the desired ethanol concentration and/or free Ca_i^{2+} flowing from a computer-controlled, pressurized system (ALA Scientific Instruments, Westbury, NY). Deionized, 100% pure ethanol (American Bioanalytical, Natick, MA) was freshly diluted in bath solution immediately before experiments. Perfusion with urea isosmotically replacing ethanol was used as the control perfusion. Even when applied at maximally effective concentration (100 mM), ethanol failed to modify the bath solution pH, as predicted from the very weak acid properties of the alcohol: pH = 7.376 ± 0.004, 7.375 ± 0.003, and 7.364 ± 0.004 for bath solution, bath solution plus 100 mM urea, and bath solution plus 100 mM ethanol, respectively ($n = 35$). Isosmotic control solution had no effect on mslo channel P_o ($n = 11$). Iberiotoxin (Alomone) was applied to the extracellular side of outside-out (O/O) patches. The electrode and bath

solutions used in O/O recordings corresponded respectively to the bath and electrode solutions described above with I/O recordings. Experiments were carried out at room temperature.

Both macroscopic and unitary currents were acquired using an EPC8 (HEKA, Lambrecht/Pfalz, Germany) amplifier and digitized using a 1320 interface and pClamp8 or pClamp9 software (Molecular Devices, Sunnyvale, CA). Macroscopic currents were evoked from I/O macropatches held at −80 mV by 200-ms, 10-mV depolarizing steps from −100 to 100 (or 160) mV. Currents were low-pass-filtered at 1 kHz with an eight-pole Bessel filter (Frequency Devices, Haverhill, MA) and sampled at 5 kHz. Average current amplitude was determined 175 to 200 ms after the start of the depolarizing step. Unitary currents were low-pass-filtered at 7 to 10 kHz with an eight-pole Bessel filter and sampled at 35 to 50 kHz.

Kinetic Modeling and Analysis

Macroscopic conductance (G)-voltage plots were fitted to a Boltzmann function of the type $G(V) = G_{max}/1 + \exp[(−V + V_{1/2})/k]$. The effective valence (z) was calculated from: $1/slope = RT/zF$, where F = 96,485 C/mol, R = 8.31 J/(mole × K), and T = absolute temperature. Data were fitted to a voltage-dependent Monod-Wyman-Changeux (VD-MWC) for allosteric proteins, using the equation

$G/G_{max} = 1/\{1 + [(1 + Ca_i^{2+}/K_C)/(1 + Ca_i^{2+}/K_O)] \times L_0 \times \exp[(−QFV)/(RT)]\}$, where G is the macroscopic conductance, Q is the gating charge, L_0 is the closed/open equilibrium constant in the absence of ligand, K_C is the Ca^{2+} dissociation constant in the closed-channel conformation, and K_O is the Ca^{2+} dissociation constant in the open-channel conformation. In this VD-MWC model, four parameters of channel gating are obtained: two are Ca^{2+}-independent (Q, L_0) and two are Ca^{2+}-dependent (K_C and K_O) (Cox and Aldrich, 2000). An ad hoc routine (Boltzmann-type of fitting), written and generously provided by Dr. Daniel Cox (Tufts University School of Medicine), was run through Igor-Pro 5 (Wave-Metrics, Lake Oswego, OR), and K_O, K_C, L_0, and Q were directly derived by fitting G/G_{max} data to the equation given above. Boltzmann fitting routines were run using the Levenberg-Marquardt algorithm to perform nonlinear least-squares fittings.

Single-channel analysis was initially performed using pClamp9 (Molecular Devices). The product of the number of channels in the patch (N) and the probability that a channel is open (P_o) was used as an index of channel steady-state activity. NP_o was calculated from the area under the curve of the Gaussian fit of all-points amplitude histograms. From a Poisson distribution of histogram data resulting from the independence and identical behavior of channel gating, $NP_o = x$i, with i = 1…n, where n is the maximum number of simultaneous conducting channels during the observation period, and x is the area under the curve corresponding to each opening, as explained in our first study of ethanol action on mslo channels (Dopico et al., 1996, 1998). This method of NP_o calculation allowed us to easily identify 1) BK_{Ca} channels from contaminant ion channels that could be present in the cell membrane, avoiding the use of blockers, and 2) possible subconductance states through which the BK_{Ca} channel might sojourn. If present, the method would have determined the contribution of these subconductances to the total channel activity and their possible modulation by calcium and/or ethanol. NP_o values were obtained from gap-free recording of single channel activity for 1 to 3 min under each condition (control bath, ethanol, washout for any given ionic gradient).

From patches where $N = 1$, dwell-time histograms were constructed using the half-amplitude threshold criterion from data low-pass-filtered at 5 to 10 kHz, rendering an effective dead time for event analysis that ranged from 18 to 28 μs. A maximum-likelihood minimization routine was used to fit exponential curves to the distribution of open and closed-times. An F table ($P < 0.01$) was used to determine the minimum number of exponential components to appropriately fit dwell-time histogram data. The number of components in the exponential fit

to the open (closed) time distribution provided a minimum estimate of the number of open (closed) states in which the channel population sojourns (Colquhoun and Hawkes, 1983). Kinetic modeling and derivation of individual rate constants were obtained using the QuB program (http://www.qub.buffalo.edu).

For the construction of a simple kinetic model of channel behavior, digitized data were first idealized using the segmental *k*-means algorithm, which uses hidden-Markov models to find the most likely sequence of events in the data set and estimate model parameters. A maximum likelihood interval analysis method was used to compute the likelihood of the experimental series of open and closed times for a given set of trial rate constants and to search for the rate constants maximizing the likelihood algorithms.

Both macroscopic and microscopic data are expressed as mean ± S.E.M., where *n* = number of patches/cell. Analysis of variance and Bonferroni's test were conducted using Instat 3.05 (GraphPad Software), and further data plotting and fitting were performed using Origin 7.0 (OriginLab Corp., Northampton, MA).

Computational Modeling

The sequences of calmodulin (PDB entry 1CLL) and the two high-affinity Ca^{2+}-binding sites of slo1 were aligned to match the first Ca^{2+}-interacting acidic residue (Asp56 in calmodulin, Asp362 in the RCK1 domain, and Glu912 in the calcium bowl), and models of both slo1 calcium binding sites were constructed using the homology modeling feature in MOE 2006.05 (Chemical Computing Group, Montreal, QC, Canada). Calcium and ethanol positions were transferred directly from the calmodulin crystal structure. The RCK1 domain model was modified to coordinate Asp367 to the calcium ion by applying distance constraints during geometry optimization of residues 366 to 368, with other atoms in the model held fixed using the MMFF94 force field.

Results

Ethanol Modulation of Channel Activity Depends on Ca_i^{2+}

We first studied ethanol action on brain BK_{Ca} (mslo) channel steady-state activity (NP_o) in the presence of highly buffered, physiological levels of free Mg_i^{2+} (1 mM) and Ca_i^{2+} (1 μM), two metal ligands that gate the BK_{Ca} channel and thus increase its NP_o (Shi et al., 2002; Xia et al., 2002). Short-term exposure of the cytosolic side of I/O patches expressing mslo to 100 mM ethanol, a maximally effective alcohol concentration on native and recombinant (slo1) BK_{Ca} channels (Dopico et al., 1998; Brodie et al., 2007), robustly increased NP_o (Fig. 1A, middle trace) in seven of seven cells; average NP_o reached 260 ± 22% of control ($p < 0.01$) (Fig. 1B) and returned to pre-ethanol values (99 ± 18% of control; $n = 7$) within 3 to 4 min after washing in an alcohol-free solution. Activating Ca_i^{2+} seemed sufficient for ethanol to increase NP_o, as ethanol action was observed in Ca^{2+}-containing, Mg^{2+}-free solutions (Fig. 1A, bottom trace). In contrast, ethanol action was lost in internal medium containing physiological levels of Mg^{2+} but no Ca^{2+} (Fig. 1A, top trace; averages given in Fig. 1B). Therefore, physiological levels of activating Ca_i^{2+}, but not physiological Mg_i^{2+}, are necessary for ethanol to increase channel activity.

To begin to determine the mechanisms underlying ligand dependence of ethanol action, we next probed ethanol on channel function across a wide voltage range, and at Ca_i^{2+} obtained in neurons under physiological or pathological conditions (Verkhratsky, 2005). Confirming an early observation (Dopico et al., 1998), ethanol potentiated BK_{Ca} currents at submicromolar levels of Ca_i^{2+} (Fig. 2A, top), with the drug effect diminishing as Ca_i^{2+} increased. Remarkably,

ethanol consistently inhibited currents when Ca_i^{2+} ranged from 10 to 100 μM (Fig. 2A, bottom). Ethanol "dual" (activation versus inhibition) effects on mslo current were also obtained when the drug was probed at 50 mM (Fig. 3); these concentrations are submaximal (~EC_{75}) to activate neuronal BK_{Ca} channels (Dopico et al., 1998; Brodie et al., 2007) and are reached in circulation in humans after moderate to heavy episodic alcohol consumption (Thombs et al., 2003).

Ethanol caused a leftward (current potentiation) or rightward (current reduction) shift in the normalized macroscopic current conductance (G/G_{max})-voltage (V) relationship (Fig. 2B). The resulting half-maximal voltage ($V_{1/2}$)-Ca^{2+} plots show that the "crossover" from ethanol activation (decrease in $V_{1/2}$) to inhibition (increase in $V_{1/2}$) occurs at ~10 μM free Ca_i^{2+} (Fig. 2C), which is also shown in G/G_{max} versus Ca_i^{2+} plots at any given voltage (Fig. 2D). As a first approximation to understand ethanol modulation of channel gating, we fitted macroscopic current data to a VD-MWC model (Cox and Aldrich, 2000). Ethanol significantly modified the two Ca^{2+}-dependent parameters of the model: the open channel-Ca^{2+} dissociation constant (K_O) and the closed channel-Ca^{2+} dissociation constant (K_C). In contrast, ethanol failed to alter the other two parameters of the model: the closed-to-open equilibrium constant in the absence of Ca^{2+} (L_0), which reflects constitutive gating, and the gating charge (Q) (Supplemental Fig. S1), both of which are Ca^{2+}-independent (Cox and Aldrich, 2000). Ethanol's lack of action on the channel gating charge is evident from identical aspects of the $V_{1/2}$ versus Ca^{2+} plots before and after factoring Q (Figs. 2E versus 2C). The unmodified gating charge is consistent with the parallel shifts along the voltage axis in the G/G_{max}-V plots regardless of ethanol potentiated or inhibited current (Fig. 2B); at any given Ca_i^{2+}, the channel effective valence (z) obtained from these plots (*Materials and Methods*) was not different between control and ethanol (e.g., at 1 μM Ca_i^{2+}, $z = 0.34 \pm 0.01$ versus 0.33 ± 0.02; $n = 9$, $p > 0.5$). Therefore, whether activating or inhibiting current, ethanol does not alter the amount of effective charge that gates the channel.

The ethanol actions on macroscopic currents in 1 mM free Mg_i^{2+} described above were identical to those in Mg^{2+}-free solution (Fig. 4), buttressing the idea that physiological Mg^{2+} is not necessary for ethanol to modulate BK_{Ca} channel gating. Collectively, our data indicate that modulation of BK_{Ca} currents by clinically relevant concentrations of ethanol is dependent on selective targeting of Ca^{2+}-driven gating.

From G/G_{max} versus Ca_i^{2+} plots (e.g., Fig. 2D), we determined the maximal effect (E_{max}; $G/G_{max} = 1$), the *apparent* dissociation constant ($K_{D(apparent)}$, in μM), and the equivalent to the Hill coefficient (n_H) for Ca^{2+} in both the absence and presence of ethanol: E_{max}, 0.98 ± 0.01 versus 0.93 ± 0.01 ($p < 0.01$); $K_{D(apparent)}$, 6.32 ± 0.17 versus 4.95 ± 0.18 ($p < 0.0001$); n_H, 3.84 ± 0.21 versus 2.55 ± 0.15 ($p < 0.0001$) ($n = 9$). Data demonstrate that the "efficacy" of the channel natural ligand (i.e., Ca^{2+}) is reduced in the presence of ethanol. In the absence of changes in the number of channels present in the membrane (Dopico et al., 1998), the decreased n_H and E_{max} for Ca^{2+} caused by short-term ethanol exposure can be explained by 1) ethanol reduction in unitary current amplitude (this would be more evident as ethanol modulation of Ca^{2+}-driven gating that leads to increased P_o reaches a "ceiling effect" at high Ca^{2+}) and/or 2) ethanol favoring ligand (Ca^{2+})-driven desensitization. To address these possibilities, we next evaluated the actions of ethanol at the single-channel level.

Ethanol Effects on Current Result from Modulation of Ca^{2+}-Driven Kinetics

Single-channel data obtained at different Ca_i^{2+} and constant voltage (60 mV) and free Mg_i^{2+} (1 mM) clearly show that ethanol failed to modify unitary current (i) amplitude (Figs. 1 and 5,

A–D). The lack of change in i was observed within a wide voltage range (−40 to +120 mV), rendering slope conductances (γ) for the ohmic section of the i/V relationship in symmetric 130 mM K^+ of 219 ± 21 and 221 ± 22 pS in control and ethanol, respectively (Supplmental Fig. S2A). Ethanol also failed to introduce subconductances during channel openings (Fig. 5, B and D). In addition, ethanol did not alter the high selectivity of the BK_{Ca} pore for K^+ over Na^+, as determined from the lack of change in Nernst potential shift when Na^+ substituted for K^+ (Supplemental Fig. S2A). This ethanol failure to modify slope conductance and Nernst shift were consistently observed under a wide variety of divalent conditions: 0.3 μM Ca^{2+} (Supplemental Fig. S2A), at which ethanol potentiates activity; 30 μM Ca^{2+} (Supplemental Fig. S2B), at which ethanol reduces activity; physiological (Supplemental Fig. S2, A and B) or 0 Mg^{2+} (Supplemental Fig. S2C). The lack of ethanol action on channel K^+ permeability and selectivity over Na^+ strongly suggests that the drug does not modify the conformation of the channel protein region involved in ion conduction. Moreover, the lack of ethanol action on channel conduction, together with ethanol failure to modify channel intrinsic gating (Fig. S1), indicates that ethanol is not acting as a solvent that alters the overall conformation of the mslo channel protein.

The dual ethanol effects on macroscopic current (Fig. 2) were paralleled by dual actions on P_o: e.g., potentiation at 0.3 μM Ca_i^{2+} (Fig. 5, A versus B) and inhibition at 30 μM Ca_i^{2+} (Fig. 5, C versus D). Thus, in the absence of changes in N and γ, ethanol effects on current are caused by drug-induced modification of P_o. Dwell-time analysis (Fig. 6) and empiric kinetic modeling (Fig. 7) explain ethanol's dual actions on P_o. At low Ca_i^{2+} (0.3 μM), both open- and closed-time distributions could be well fit to triple exponentials, suggesting the existence of at least three open and three closed channel states. At 30 μM Ca_i^{2+}, however, the channel enters a low-activity mode of gating, which can be seen in single-channel recordings low-pass-filtered at 1 kHz as interburst periods of very low P_o lasting hundreds of milliseconds (Fig. 5, C and D). At the bottom of each panel, time-expanded records low-pass-filtered at 7 kHz demonstrate that this low-activity mode includes flickery openings (arrows), resulting in an additional closed time life of ~3 ms. Thus, at 30 μM Ca_i^{2+}, the closed time distribution could be satisfactorily fit to four exponentials (Fig. 6). These data with mslo channels support a previous study with native BK_{Ca} channels reporting that $Ca_i^{2+}>10 \mu$M drives channel entry into a complex, low-activity mode (Rothberg et al., 1996).

At submicromolar Ca_i^{2+} levels, ethanol drastically decreased channel long-closed events (τ_{C2} and τ_{C3}). In addition, ethanol increased the probability of occurrence of long open events (τ_{O3}) (Fig. 6). These ethanol actions on channel time-lives are similar to those of Ca^{2+} (Rothberg et al., 1996) and explain the resulting increase in P_o at $Ca_i^{2+}<10 \mu$M. On the other hand, ethanol reduction of P_o at 30 μM Ca_i^{2+} (Fig. 5, D versus C) is determined by a robust reduction in the average duration of long-open events (τ_{O3}) and, more significantly, a major increase in both duration and probability of occurrence of long-closed events (τ_{C3} and τ_{C4}) (Fig. 6), as the channel spends more time in the low-activity mode (see time-expanded traces in Fig. 5, D versus C). Thus, ethanol facilitates channel dwelling in a low-activity mode, resembling the actions of high micromolar Ca^{2+} on channel behavior (Rothberg et al., 1996).

Empiric, simple kinetic models explain in more detail how ethanol favors channel dwelling into the low-activity mode (Fig. 7). Based on the number of exponentials used to properly fit the dwell-times distribution without over-parametization (see *Materials and Methods*), we started our kinetic channel modeling by considering three open and three closed states, this initial input model (control, 0.3 μM Ca^{2+}) having 12 rate constants. Optimization of data by QuB rendered the models shown in Fig. 7, A and B. It is noteworthy that we could only model

the channel behavior at high Ca_i^{2+} satisfactorily by introducing an additional "state" (low-activity mode; Fig. 7, C versus A). Therefore, final (optimized) models for control and ethanol in 30 μM Ca^{2+} contain 7 "states" and 14 rate constants (Fig. 7, C and D) (other formalism such as the differential equations used and their corresponding matrices are given as Supplemental Information, online). Comparison of these optimized models shows that ethanol mildly diminishes the C3→C2 transition within the normal gating mode and drastically shifts the equilibrium between C3 and the low-activity mode toward the latter ($\times$ ~5 times) (Fig. 7, D versus C). These drug actions effectively favored the probability of the channel dwelling in the low-activity mode, from <5% to >10% in the absence and presence of ethanol. This change, together with a decrease in the probability to dwell in open states of intermediate duration (O_2) results in an overall decrease in P_o (for P_o derivation from the kinetic rate constants used in the optimized models, please also see Supplemental Data; online). Ethanol actions on rate constants within the "normal" gating mode, which explain the ethanol increase in P_o at submicromolar levels of Ca_i^{2+}, are described in the Fig. 7 legend. In brief, ethanol increase in P_o results from the drug increasing the probability of the channel dwelling in O2 and decreasing the probability of the channel dwelling in C3 (Supplemental Information; online).

A fact that contributes to the simplicity of the models shown in Fig. 7 is that they include only variant Ca_i^{2+} in the presence or absence of ethanol. Others determinants of gating, such as constitutive activity, Mg_i^{2+}, and gating charge, have not been considered because they do not interfere with ethanol action (Figs. 2 and 4 and Supplemental Fig. S1). The models, while simple, appropriately describe the ethanol-Ca^{2+} interaction and its overall effect on P_o. First, at all conditions (low and high Ca_i^{2+}, absence or presence of ethanol), P_o values calculated from the model rate constants are similar to those determined experimentally from all-points amplitude histograms (compare P_o values in the caption of Fig. 7 versus those in Fig. 5). Second, we ran our models and obtained simulated single-channel records (Fig. S3) that look practically identical to those obtained experimentally at all conditions (Fig. 5). Collectively, dwell-time histogram analysis and kinetic modeling seem to indicate that, whether the overall effect is increased P_o (at Ca_i^{2+}<10 μM) or decreased P_o (at Ca_i^{2+}>10 μM), ethanol's final effect on mslo activity results primarily from facilitation of Ca^{2+}-driven events and kinetic transitions. Our single-channel data and analysis, together with the lack of ethanol action on constitutive activity and voltage-driven gating (Fig. 2), and the necessity of physiologically activating Ca_i^{2+} (but not Mg_i^{2+}) for ethanol effects on current led us to conclude that the drug, at concentrations that maximally modify slo1 channel function and current (Dopico et al., 1998;Brodie et al., 2007), cannot gate the channel in the absence of Ca_i^{2+}. Ethanol (a "coagonist") works as a selective *adjuvant* of activating Ca_i^{2+} (the agonist), which results in current potentiation or inhibition at low and high agonist concentrations, respectively.

Our results underscore a fundamental interaction among two ligands (Ca_i^{2+} and ethanol) and a simple receptor system:the BK_{Ca}-forming mslo subunit and its immediate proteolipid environment. Although homotetrameric slo1 channels seem to exist in some tissues (Papassotiriou et al., 2000), most brain BK_{Ca} channels consist of the association of slo1 and accessory subunits of the β_4 subtype (Brenner et al., 2000; Salkoff et al., 2006). Thus, we probed next whether the fundamental interaction among Ca_i^{2+}, ethanol and mslo sub-units that is reflected by a Ca_i^{2+}-dependent dual modulation of current by the alcohol is modified by the presence of neuronally abundant BK_{Ca} β_4 subunits.

The functional expression of a BK_{Ca} β_4 subunits was determined by the refractoriness of the nslo+β_4 heteromeric channel to iberiotoxin block in O/O patches, in contrast to the sensitivity

of homomeric slo1 channels to this peptidyl blocker (data not shown) (Bukiya et al., 2007, 2008). At 0.3 μM Ca_i^{2+}, exposure to 100 mM ethanol consistently increased mslo+β_4 channel NP_o (Supplemental Fig. S4, B versus A, and E). At 30 μM Ca_i^{2+}, however, 100 mM ethanol caused a mild but significant decrease in mslo+β_4 channel NP_o (Supplemental Fig. S4, D versus C, and E). This alcohol dual action on channel NP_o occurred in absence of changes in unitary current amplitude (Supplemental Fig. S4, A–D). Collectively, these data clearly indicate that within physiological calcium levels (0.3–30 μM Ca_i^{2+}), the presence of functional BK_{Ca} β_4 subunits does not drastically modify ethanol pattern of modulation of slo1 channel activity (but see *Discussion*).

Structural Domains in slo1 That Determine Ethanol Facilitation of Ca^{2+}-Driven Gating

After determining that ethanol action on BK_{Ca} currents results from alcohol-specific facilitation of Ca^{2+}-driven gating of the slo channel, we set to determine which functional domains in the slo1 subunit are involved in this fundamental alcohol action. Slo1 channels sense activating Ca^{2+} through at least three recognition sites, which can be distinguished based on their differential selectivity for divalents and Ca^{2+} affinities: 1) the calcium-bowl region includes residues Glu912 and Asp923, thought to contribute to divalent coordination, and a penta-aspartate sequence (the 5D5N mutation drastically diminishes the Ca^{2+} sensitivity of the slo1 channel (Bian et al., 2001; Bao et al., 2004; Sheng et al., 2005; Salkoff et al., 2006); 2) the high-affinity "site" in the RCK1 domain corresponds to Asp362 and Asp367, which are thought to coordinate divalents (Xia et al., 2002); and 3) the low-affinity "site" in the RCK1 domain, determined by Glu374 and Glu399 (Shi et al., 2002). The first two sites selectively discriminate Ca^{2+} over Mg^{2+}, and nonconserved mutations in these sites drastically reduce the channel activation by low micromolar levels of Ca_i^{2+}. In contrast, the third site responds to activation by hundreds of micromolar Ca^{2+} and millimolar Mg^{2+} (Zeng et al., 2005).

Ca^{2+} bowl 5D5N channel mutants were characterized by a significant decrease in apparent Ca_i^{2+} sensitivity, which is evident from the right-shift in the $V_{1/2}$- Ca_i^{2+} plot compared with that of *wt* mslo (Fig. 2B). Ethanol, however, still caused channel activation and inhibition at low and high Ca_i^{2+} levels (Fig. 8A), as it did in *wt mslo*, indicating that a functional Ca^{2+} bowl is not necessary for drug action on *slo1* channels. In contrast, the D362A/D367A mutation (Xia et al., 2002) abolished ethanol inhibition ($n = 8$) yet did not modify ethanol potentiation (Fig. 8B). This finding indicates the involvement of the RCK1 high-affinity site in the Ca^{2+}-ethanol interaction that leads to decreased P_o. Because this decrease was due to facilitation by ethanol of channel dwelling in a low-activity mode (Figs. 5 and 7), ethanol results with the D362A/D367A mutant led us to hypothesize that 1) at $Ca_i^{2+} \gg 10\,\mu$M, the D362A/D367A mutant fails to enter a low-activity mode and 2) ethanol fails to reduce $(N)P_o$ in this mutant. Single-channel data correctly prove both hypotheses (Supplemental Fig. S5). Thus, the RCK1 high-affinity site is sufficient to mediate the ethanol-calcium interaction that results in decreased P_o. Because ethanol inhibition remained in both the calcium bowl and the RCK low-affinity site mutant (Fig. 8C), it seems that the RCK1 Asp362/Asp367 site is not only sufficient but also necessary for this ethanol action.

On the other hand, mutations in each of the sites that participate in sensing micromolar physiological levels of Ca_i^{2+} failed to modify ethanol-induced potentiation (Fig. 8, A and B). However, combining the 5D5N with the D362A/D367A mutations not only suppressed ethanol-induced inhibition (as found with the D362A/D367A mutant itself), but also consistently abolished (eight of eight cells) ethanol activation (Fig. 8D). These data were obtained in 1 mM free Mg_i^{2+} and 100 μM free Ca_i^{2+}, a divalent concentration that seems

sufficient to gate the channel (Xia et al., 2002; Zeng et al., 2005). Even when Ca_i^{2+} was raised to 1 mM, the combined 5D5N, D362A/D367A mutant failed to be activated by ethanol (Supplemental Fig. S6). Together, data from Fig. 8, A–C, indicate that neither a functional Ca^{2+} bowl nor a functional RCK1 high-affinity site is necessary for ethanol-induced activation, yet each domain is sufficient for supporting this drug action.

Finally, consistent with the failure of millimolar Mg_i^{2+} to modulate ethanol actions (Figs. 1 and 4), the mutations E374A/E399A failed to modify BK_{Ca} activation or inhibition by ethanol (Fig. 8C). In conclusion, as far as submicromolar-low micromolar Ca_i^{2+}, the channel-specific and natural ligand, is sensed by one of its two high-affinity sites in the slo1 protein, ethanol modulates channel gating. In absence of slo1 crystallographic data, structural insights into the Ca_i^{2+}-ethanol interactions on these slo1 high-affinity sites remain largely speculative. Crystal structures of apocalmodulin and Ca^{2+}-bound calmodulin in the presence and absence of ethanol (Chattopadhyaya et al., 1992) provide a precedent for an ethanol binding site created upon Ca^{2+} binding. This model of Ca^{2+}-dependent ethanol binding may be applicable to slo1 and thus explain the requirement of Ca^{2+} presence for ethanol to modulate slo1 P_o, as explored under *Discussion*.

Discussion

Our study demonstrates that ethanol at concentrations that are maximally effective to modify neuronal BK_{Ca} currents and, thus, excitability, brain function, and behavior (Gruss et al., 2001; Martin et al., 2004; Brodie et al., 2007) can modulate slo1 channel activity only in the presence of activating Ca_i^{2+}. Furthermore, ethanol actions depend on the concentrations of this activating ligand. As summarized in Fig. 9, at submicromolar to low micromolar levels of Ca_i^{2+}, the equilibria from nonconducting to conducting states as a result of Ca^{2+} binding to the calcium bowl or the RCK1 high-affinity site present in the slo1 subunit are shifted by ethanol, rendering increased P_o and thus macroscopic current. The equilibrium from the channel "normal" gating mode to a low P_o mode is favored by higher Ca_i^{2+} and involves the RCK1 high-affinity binding site. This transition is favored by ethanol, diminishing overall P_o and thus current. In contrast, ethanol seems not to modify gating transitions involving divalent recognition by the RCK1 low-affinity site or movement of gating charge. In addition, ethanol fails to modify the channel intrinsic gating and ion conduction properties. Therefore, ethanol is not changing channel function by altering the overall conformation of the slo1 protein or the arrangement of the slo1 subunits in a functional tetrameric channel. Instead, ethanol action is that of a facilitator of the specific natural ligand that gates the channel (i.e., Ca_i^{2+}).

A distinct feature of BK_{Ca} channel gating is that both independent and synergistic activation by transmembrane voltage and Ca_i^{2+} can occur (Cox and Aldrich, 2000; Niu et al., 2004). Synergism and independence in BK_{Ca} gating are determined by the summation of forces at the channel S6 gate, resulting from the coupling of both voltage sensors (S4) and the several Ca^{2+} sensors to the gates via peptidic "springs" in the channel structure (Niu et al., 2004). In the absence of Ca^{2+}, a linear relationship between P_o and spring distance is consistent with the linker-gating ring acting as a passive spring attached to the S6 gate (Niu et al., 2004). Evidence that ethanol 1) does not modify voltage-driven (Fig. 2 and Supplemental Fig. S1) or 2) Mg^{2+}-driven (Fig. 4) gating and 3) cannot gate the channel in the absence of Ca^{2+} (Fig. 1) all seem to indicate that ethanol fails to modify the behavior of the passive spring attached to the S6 gate. On the other hand, we show that ethanol action is unaffected by the absence of Mg_i^{2+} (Figs. 1 and 4) or the Glu374/Glu399 mutations (Fig. 8C), which define the Mg^{2+} recognition site (Shi et al., 2002). The lack of ethanol interactions with voltage- and Mg^{2+}-driven gating

is consistent with the idea that slo1 channel gating driven by these two biological signals may be coupled (Hu et al., 2003).

Rather, it is Ca^{2+} sensing by either the calcium bowl or the RCK1 high-affinity site that allows ethanol to modulate P_o and thus current. It is noteworthy that both these sites (but not the Glu374/Glu399 site) can sense and participate in gating driven by low micromolar Ca^{2+} but not millimolar Mg_i^{2+} (Shi et al., 2002; Zeng et al., 2005). To obtain structural insights into the Ca^{2+} dependence of ethanol action, homology modeling of the calcium bowl and RCK1 high-affinity sites was performed. The most relevant structural template for ethanol interaction with a Ca^{2+}-binding protein is calmodulin. Supplemental Fig. S7A demonstrates that ethanol per se does not have any effect on the apocalmodulin domain folding, which is modified solely upon Ca^{2+} binding. Ethanol is positioned in a groove near the amino end of an α-helix and not far away from the Ca^{2+}-coordinating residues. Remarkably, ethanol is present only when Ca^{2+} is bound to the metal coordinating residues.

To determine the relevance of this template to the high-affinity Ca^{2+}-binding sites in slo1, sequences were aligned to match the first Ca^{2+}-interacting acidic residue (*Materials and Methods*). The slo1 calcium bowl and RCK1 high-affinity site models include ethanol located in a groove between two α-helices and near their amino ends, not far away from the Ca^{2+}-coordinating residues (Supplemental Fig. S7B). The ethanol location is near but not identical to that of activating Ca^{2+}. Thus, although some kinetic actions of both ligands overlap (Fig. 5–7), Ca^{2+} and ethanol should be considered heterotropic ligands of the slo1 channel. Ethanol is near a region that allows hydrogen bonding. This pattern is common to several proteins whose activity is modulated by ethanol (Dwyer and Bradley, 2000). This location predicts that more efficient hydrogen bond donor/acceptors than ethanol will interact more efficiently than ethanol will. Consistent with this, trichloroethanol effects on BK_{Ca} channel activity and AP in dorsal root ganglia group-A neurons are more robust than those of ethanol (Gruss et al., 2001).

Ethanol increases Ca^{2+}-binding to calmodulin (Ohashi et al., 2004). It is conceivable that an equivalent ethanol location in slo1 high-affinity binding sites could also increase their affinity for the metal and thus facilitate Ca^{2+}-driven gating, as demonstrated by the changes in K_C/K_O (Fig. 2 and Supplemental Fig. S1), P_o (Fig. 5), and kinetic analysis (Figs. 6 and 7). Application of the apocalmodulin/calmodulin model to slo1 high-affinity site Ca^{2+}-dependent ethanol binding might also explain why ethanol per se cannot activate the channel (i.e., cannot substitute for activating Ca_i^{2+}), because ethanol does not have any effect on domain folding. Finally, the residue responsible for the Ca^{2+}-induced conformational change in calmodulin (Glu67) has a homolog in the slo1 calcium bowl (Asp923). The RCK1 high-affinity site, however, lacks an acidic residue at the top of the C-terminal helix. Thus, the calcium-induced conformational changes reported for calmodulin are likely to be followed more closely by those in the calcium bowl than those in the RCK1 high-affinity site. On the other hand, the RCK1 high-affinity site, but not the calcium bowl, determines ethanol-induced reduction in P_o at high micromolar Ca^{2+} (Fig. 8, A and B). It is noteworthy that the contribution of these two sites to the slo1 gating process is not identical; macroscopic kinetic analysis shows that the Asp362/Asp367 site, but not the calcium bowl, slows slo1 channel deactivation at 10 to 300 μM Ca_i^{2+} (Zeng et al., 2005). It might be possible that the RCK1 high-affinity site favors both slow deactivation and entry into a desensitized state(s) or low-affinity mode from a common kinetic state(s) (e.g., C3 in Fig. 7). From our data, it is clear that the D362A/D367A mutant fails to enter the low-activity mode and, accordingly, is not inhibited by ethanol (Supplemental Fig. S5).

Among members of the TM6 K^+ channel superfamily, slo1 presents a unique, high sensitivity to ethanol (EC_{50}, ~25 mM; E_{max}, ~100 mM; Dopico et al., 1998; Liu et al., 2006). We show that this sensitivity is secondary to ethanol modulation of Ca^{2+}-driven gating determined by Ca^{2+} interactions with the calcium bowl and the RCK1 high-affinity site, two structures missing in voltage-gated K^+ channels other than slo1 (Salkoff et al., 2006). In addition, slo1 distinctively contains an extra segment (S0), rendering an exofacial N-end (Salkoff et al., 2006). CamKII-induced phosphorylation of Thr107 in the S0-S1 linker of bovine aorta slo1 (bslo) channels (which share all relevant Ca^{2+} sensing sites with mslo mbr5) can gradually switch ethanol responses from activation to inhibition. These data were obtained at $Ca_i^{2+} < 10\,\mu M$, indicating that phosphorylation of Thr107 in bslo can override ethanol amplification of Ca^{2+} activation of slo1, and suggest a functional coupling between the S0-S1 linker and the Ca^{2+}-sensing sites involved in the Ca^{2+}-ethanol interaction.

Our study identifies a functional interaction between ethanol and Ca_i^{2+} that occurs at the BK_{Ca} channel-forming slo1 subunit. The final ethanol effect on BK_{Ca} channel gating, however, should be fine-tuned by accessory proteins that control the Ca^{2+} sensitivity of the channel complex. In particular, BK_{Ca} beta$_1$ subunits drastically increase the apparent Ca^{2+} sensitivity of slo1 channels (Brenner et al., 2000; Cox and Aldrich, 2000; Nimigean and Magleby, 2000). According to our model, an increase in apparent Ca_i^{2+} sensitivity should facilitate agonist-mediated channel dwelling into the low-activity mode (which is further favored by ethanol presence; Fig. 7), diminishing ethanol potentiation. Heterologous coexpression of β_1 subunits consistently reduces ethanol potentiation of hslo channels (Feinberg-Zadek and Treistman, 2007).

In the brain, most native BK_{Ca} channels consist of the association of slo1 and β_4 subunits (Brenner et al., 2000; Weiger et al., 2002). Within physiological levels of Ca_i^{2+} found in neurons (0.3–30 μM), the presence of β_4 subunits did not modify the basic fundamental interaction between ethanol and Ca_i^{2+}. However, the degree of ethanol-induced potentiation observed at submicromolar Ca_i^{2+} was diminished by β_4. In addition, the ethanol-induced inhibition observed at 30 μM Ca_i^{2+} was somewhat increased by β_4 (Supplemental Fig. S4, C–E versus Fig. 5, C and D). This pattern is consistent with the fact that β_4 produces a very modest shift in apparent Ca^{2+}-sensitivity within the low micromolar to 30 μM Ca_i^{2+} range (Wang et al., 2006) and likely explains data showing some modulation of alcohol action on hslo channels by β_4 subunits (Feinberg-Zadek and Treistman, 2007). In brief, in the presence of Ca_i^{2+} at resting levels ($Ca_i^{2+} \leq 10\,\mu M$), our ligand-adjuvant mechanism predicts that ethanol will potentiate BK_{Ca} currents in neurons. Indeed, this is a widespread finding (Brodie et al., 2007). On the other hand, overall Ca_i^{2+} in neurons can reach several tens of micromolar during pathophysiological processes, including excitotoxicity, seizures, and aging (Tymianski and Tator, 1996). At these Ca_i^{2+} levels, ethanol will inhibit BK_{Ca} channels, impairing one of the major channel populations that protects a cell from toxic Ca_i^{2+} levels (Han et al., 2007).

Differential subunit coexpression could contribute to the relative refractoriness of native BK_{Ca} channels in nucleus accumbens neuronal dendrites to ethanol activation compared with their counterparts in the somata. The somatic channels express both β_1 and β_4 subunits, whereas the dendritic channels express primarily β_1 (Martin et al., 2004). When evaluated within a Ca_i^{2+} range at which β_1-subunit coupling to slo1 effectively translates into increased P_o (Nimigean and Magleby, 2000) (i.e., increased apparent Ca_i^{2+} sensitivity), the dendritic BK_{Ca} channels are indeed more Ca_i^{2+}-sensitive than their somatic counterparts (Martin et al.,

2004). Likewise, native BK_{Ca} channels in the somata versus nerve endings of supraoptic neurons display different current phenotypes, including apparent Ca_i^{2+} sensitivity, consistent with functional expression of slo1+β_1 subunits in the somata, and expression of slo1+β_4 in the nerve endings. It is noteworthy that these nerve-ending BK_{Ca} channels are sensitive to clinically relevant alcohol concentrations, whereas the somata channels are not (Brodie et al., 2007).

Clinically relevant concentrations of ethanol can modify independently of cell integrity the activity of the vast majority of ligand-gated ion channels (Lima-Landman and Albuquerque, 1989; Lovinger et al., 1990; Wu and Miller, 1994; Parker et al., 1996; Valenzuela et al., 1998; Aistrup et al., 1999; Beckstead et al., 2002; Trevisani et al., 2002; Zhang et al., 2002; Möykkynen et al., 2003; Wallner et al., 2003; Davies et al., 2005). Among inwardly rectifying channels, only G protein-activated K^+ channels (Lewohl et al., 1999) are ethanol-sensitive, and among the voltage-gated TM6 K^+ channel superfamily, BK_{Ca} are highly sensitive (Dopico et al., 1998; Martin et al., 2004; Brodie et al., 2007). Thus, we speculated whether the adjuvant-ligand interpretation that we applied to our results of ethanol-Ca^{2+} interactions on BK_{Ca} could explain some functional ethanol data obtained with ligand-gated channels other than BK_{Ca}. First, our interpretation requires ethanol to modulate activity in the presence of efficacious ligand (agonist). This requirement should be overcome in constitutively active channels, because a mutation substituting for agonist-binding diminishes the energy required to drive the channel from the inactivated to the activated state (Galzi et al., 1996). Indeed, although strychnine-sensitive glycine receptors are resistant to ethanol and anesthetics in the absence of glycine, constitutively active glycine receptor mutants are sensitive to these molecules (Beckstead et al., 2002). Likewise, whereas *wt* 5-HT3 receptors are ethanol-insensitive in absence of serotonin, constitutively active 5-HT3 mutants are ethanol-sensitive (Zhang et al., 2002).

In addition, the adjuvant-ligand interpretation requires that ethanol modulation of channel activity depends on the concentration of the agonist. In channels such as slo1, where the ligand-dependent shift toward a low-activity mode or desensitized state(s) occurs only at high agonist concentrations, adjuvating the agonist with ethanol must result in ethanol-induced activation and inhibition at low and high agonist concentrations, respectively, as shown in the present study. On the other hand, in channels with minor ligand-induced desensitization, ethanol would potentiate ligand-driven activation, the potentiation being diminished as the agonist reaches maximal effect. This also was reported for the Gly receptor (Beckstead et al., 2002). In general, in ligand-gated channels that are potentiated by ethanol, the ethanol effect would diminish with agonist concentration, as found with P2X3 (Davies et al., 2005), bungarotoxin-insensitive nACh (Aistrup et al., 1999), 5-HT3 (Parker et al., 1996), and GABA-A (Wallner et al., 2003) receptors. Finally, in channels with significant desensitization processes, our interpretation predicts that ethanol will primarily reduce activity. Thus, blocking desensitization by pharmacological agents or mutations should reduce ethanol inhibition or even turn it into ethanol potentiation. These patterns were observed with *α*-amino-3-hydroxy-5-methyl-4-isoxazolepropionic acid (Möykkynen et al., 2003) and *N*-methyl-D-aspartate channels (Lima-Landman and Albuquerque, 1989), respectively.

In brief, our interpretation of ethanol action on BK_{Ca} channels might apply to several results obtained with ethanol on a wide variety of ligand-gated channels. The fundamental requirements of the model are that 1) ethanol cannot gate the channel unless an activating ligand (or a mutation substituting for it) is present and bound to the receptor channel; 2) ethanol, acting as an adjuvant of the activating ligand (agonist), may evoke differential responses in channel activity, which depend on agonist concentration; and 3) the ethanol site is different from that of the channel agonist (heterotropic ligands). Whether nearby or far away in the protein or protein-lipid interface, however, the ethanol binding site must be functionally coupled to the binding site(s) of a channel agonist.

Supplementary Material

Refer to Web version on PubMed Central for supplementary material.

Acknowledgments

ABBREVIATIONS

BK_{Ca}

large conductance calcium- and voltage-gated potassium

AP

action potential

RCK

regulation of conductance for K^+

P_o

channel open probability

O/O

outside out

I/O

inside out

VD-MWC

voltage-dependent Monod-Wyman-Changeux

References

Aistrup GL, Marszalec W, Narahashi T. Ethanol modulation of nicotinic acetylcholine receptor currents in cultured cortical neurons. Mol Pharmacol 1999;55:39–49. [PubMed: 9882696]

Bao L, Kaldany C, Holmstrand EC, Cox DH. Mapping the BKCa channel's "Ca^{2+} bowl": side-chains essential for Ca^{2+} sensing. J Gen Physiol 2004;123:475–489. [PubMed: 15111643]

Beckstead MJ, Phelan R, Trudell JR, Bianchini MJ, Mihic SJ. Anesthetic and ethanol effects on spontaneously opening glycine receptor channels. J Neurochem 2002;82:1343–1351. [PubMed: 12354281]

Bers DM, Patton CW, Nuccitelli R. A practical guide to the preparation of Ca^{2+} buffers. Methods Cell Biol 1994;40:3–29. [PubMed: 8201981]

Bian S, Favre I, Moczydlowski E. Ca^{2+}-binding activity of a COOH-terminal fragment of the *Drosophila* BK channel involved in Ca^{2+}-dependent activation. Proc Natl Acad Sci U S A 2001;98:4776–4781. [PubMed: 11274367]

Brenner R, Jegla TJ, Wickenden A, Liu Y, Aldrich RW. Cloning and functional characterization of novel large conductance calcium-activated potassium channel beta subunits, hKCNMB3 and hKCNMB4. J Biol Chem 2000;275:6453–6461. [PubMed: 10692449]

Brodie MS, Scholz A, Weiger TM, Dopico AM. Ethanol interactions with calcium-dependent potassium channels. Alcohol Clin Exp Res 2007;31:1625–1632. [PubMed: 17850640]

Bukiya AN, Liu J, Toro L, Dopico AM. Beta1 (KCNMB1) subunits mediate lithocholate activation of large-conductance Ca^{2+}-activated K^+ channels and dilation in small, resistance-size arteries. Mol Pharmacol 2007;72:359–369. [PubMed: 17468198]

Bukiya AN, Vaithianathan T, Toro L, Dopico AM. The second transmembrane domain of the large conductance, voltage- and calcium-gated potassium channel beta(1) subunit is a lithocholate sensor. FEBS Lett 2008;582:673–678. [PubMed: 18242174]

Chattopadhyaya R, Meador WE, Means AR, Quiocho FA. Calmodulin structure refined at 1.7 A resolution. J Mol Biol 1992;228:1177–1192. [PubMed: 1474585]

Colquhoun, D.; Hawkes, AG. The principles of the stochastic interpretation of ion-channel mechanisms. In: Sakmann, B.; Neher, E., editors. Single Channel Recording. Plenum Press; New York, NY: 1983. p. 135-175.

Cox DH, Aldrich RW. Role of the beta1 subunit in large-conductance Ca^{2+}-activated K^+ channel gating energetics. Mechanisms of enhanced Ca^{2+} sensitivity. J Gen Physiol 2000;116:411–432. [PubMed: 10962017]

Davies DL, Kochegarov AA, Kuo ST, Kulkarni AA, Woodward JJ, King BF, Alkana RL. Ethanol differentially affects ATP-gated P2X(3) and P2X(4) receptor subtypes expressed in *Xenopus* oocytes. Neuropharmacology 2005;49:243–253. [PubMed: 15993446]

Dopico AM. Ethanol sensitivity of BK(Ca) channels from arterial smooth muscle does not require the presence of the beta 1-subunit. Am J Physiol Cell Physiol 2003;284:C1468–C1480. [PubMed: 12570985]

Dopico AM, Anantharam V, Treistman SN. Ethanol increases the activity of Ca^{2+}-dependent K^+ (mslo) channels: functional interaction with cytosolic Ca^{2+} J Pharmacol Exp Ther 1998;284:258–268. [PubMed: 9435186]

Dopico AM, Lemos JR, Treistman SN. Ethanol increases the activity of large conductance, Ca^{2+}-activated K^+ channels in isolated neurohypophysial terminals. Mol Pharmacol 1996;49:40–48. [PubMed: 8569710]

Dwyer DS, Bradley RJ. Chemical properties of alcohols and their protein binding sites. Cell Mol Life Sci 2000;57:265–275. [PubMed: 10766022]

Feinberg-Zadek PL, Treistman SN. Beta-subunits are important modulators of the acute response to alcohol in human BK channels. Alcohol Clin Exp Res 2007;31:737–744. [PubMed: 17391339]

Galzi JL, Edelstein SJ, Changeux J. The multiple phenotypes of allosteric receptor mutants. Proc Natl Acad Sci U S A 1996;93:1853–1858. [PubMed: 8700848]

Gruss M, Henrich M, König P, Hempelmann G, Vogel W, Scholz A. Ethanol reduces excitability in a subgroup of primary sensory neurons by activation of BK_{Ca} channels. Eur J Neurosci 2001;14:1246–1256. [PubMed: 11703454]

Han X, Wang F, Yao W, Xing H, Weng D, Song X, Chen G, Xi L, Zhu T, Zhou J, et al. Heat shock proteins and p53 play a critical role in K^+ channel-mediated tumor cell proliferation and apoptosis. Apoptosis 2007;12:1837–1846. [PubMed: 17624594]

Hu L, Shi J, Ma Z, Krishnamoorthy G, Sieling F, Zhang G, Horrigan FT, Cui J. Participation of the S4 voltage sensor in the Mg^{2+}-dependent activation of large conductance (BK) K^+ channels. Proc Natl Acad Sci U S A 2003;100:10488–10493. [PubMed: 12925732]

Lewohl JM, Wilson WR, Mayfield RD, Brozowski SJ, Morrisett RA, Harris RA. G-protein-coupled inwardly rectifying potassium channels are targets of alcohol action. Nat Neurosci 1999;2:1084–1090. [PubMed: 10570485]

Lima-Landman MT, Albuquerque EX. Ethanol potentiates and blocks NMDA-activated single-channel currents in rat hippocampal pyramidal cells. FEBS Lett 1989;247:61–67. [PubMed: 2468533]

Liu J, Asuncion-Chin M, Liu P, Dopico AM. CaM kinase II phosphorylation of slo Thr107 regulates activity and ethanol responses of BK channels. Nat Neurosci 2006;9:41–49. [PubMed: 16341213]

Liu P, Xi Q, Ahmed A, Jaggar JH, Dopico AM. Essential role for smooth muscle BK channels in alcohol-induced cerebrovascular constriction. Proc Natl Acad Sci U S A 2004;101:18217–18222. [PubMed: 15604147]

Lovinger DM, White G, Weight FF. NMDA receptor-mediated synaptic excitation selectively inhibited by ethanol in hippocampal slice from adult rat. J Neurosci 1990;10:1372–1379. [PubMed: 2158533]

Martin G, Puig S, Pietrzykowski A, Zadek P, Emery P, Treistman S. Somatic localization of a specific large-conductance calcium-activated potassium channel subtype controls compartmentalized ethanol sensitivity in the nucleus accumbens. J Neurosci 2004;24:6563–6572. [PubMed: 15269268]

McManus OB. Calcium-activated potassium channels: regulation by calcium. J Bioenerg Biomembr 1991;23:537–560. [PubMed: 1917908]

Möykkynen T, Korpi ER, Lovinger DM. Ethanol inhibits alpha-amino-3-hydyroxy-5-methyl-4-isoxazolepropionic acid (AMPA) receptor function in central nervous system neurons by stabilizing desensitization. J Pharmacol Exp Ther 2003;306:546–555. [PubMed: 12734392]

Nimigean CM, Magleby KL. Functional coupling of the beta1 subunit to the large conductance Ca^{2+}-activated K^+ channel in the absence of Ca^{2+}. Increased Ca^{2+} sensitivity from a Ca^{2+}-independent mechanism. J Gen Physiol 2000;115:719–736. [PubMed: 10828246]

Niu X, Qian X, Magleby KL. Linker-gating ring complex as passive spring and Ca^{2+}-dependent machine for a voltage- and Ca^{2+}-activated potassium channel. Neuron 2004;42:45–56.

Ohashi I, Pohoreki R, Morita K, Stemmer PM. Alcohols increase calmodulin affinity for Ca^{2+} and decrease target affinity for calmodulin. Biochim Biophys Acta 2004;1691:161–167. [PubMed: 15110996]

Papassotiriou J, Köhler R, Prenen J, Krause H, Akbar M, Eggermont J, Paul M, Distler A, Nilius B, Hoyer J. Endothelial K^+ channel lacks the Ca^{2+} sensitivity-regulating beta subunit. FASEB J 2000;14:885–894. [PubMed: 10783142]

Parker RM, Bentley KR, Barnes NM. Allosteric modulation of 5-HT3 receptors: focus on alcohols and anaesthetic agents. Trends Pharmacol Sci 1996;17:95–99. [PubMed: 8936343]

Priel A, Gil Z, Moy VT, Magleby KL, Silberberg SD. Ionic requirements for membrane-glass adhesion and giga seal formation in patch-clamp recording. Biophys J 2007;92:3893–3900. [PubMed: 17369408]

Rothberg BS, Bello RA, Song L, Magleby KL. High Ca^{2+} concentrations induce a low activity mode and reveal Ca^{2+}-independent long shut intervals in BK channels from rat muscle. J Physiol 1996;493:673–689. [PubMed: 8799891]

Salkoff L, Butler A, Ferreira G, Santi C, Wei A. High-conductance potassium channels of the SLO family. Nat Rev Neurosci 2006;7:921–931. [PubMed: 17115074]

Sheng JZ, Weljie A, Sy L, Ling S, Vogel HJ, Braun AP. Homology modeling identifies C-terminal residues that contribute to the Ca^{2+} sensitivity of a BK_{Ca} channel. Biophys J 2005;89:3079–3092. [PubMed: 16100257]

Shi J, Krishnamoorthy G, Yang Y, Hu L, Chaturvedi N, Harilal D, Qin J, Cui J. Mechanism of magnesium activation of calcium-activated potassium channels. Nature 2002;418:876–880. [PubMed: 12192410]

Thombs DL, Olds RS, Snyder BM. Field assessment of BAC data to study late-night college drinking. J Stud Alcohol 2003;64:322–330. [PubMed: 12817820]

Trevisani M, Smart D, Gunthorpe MJ, Tognetto M, Barbieri M, Campi B, Amadesi S, Gray J, Jerman JC, Brough SJ, et al. Ethanol elicits and potentiates nociceptor responses via the vanilloid receptor-1. Nat Neurosci 2002;5:546–551. [PubMed: 11992116]

Tymianski M, Tator CH. Normal and abnormal ca lcium homeostasis in neurons: a basis for the pathophysiology of traumatic and ischemic central nervous system injury. Neurosurgery 1996;38:1176–1195. [PubMed: 8727150]

Valenzuela CF, Bhave S, Hoffman P, Harris RA. Acute effects of ethanol on pharmacologically isolated kainate receptors in cerebellar granule neurons: comparison with NMDA and AMPA receptors. J Neurochem 1998;71:1777–1780. [PubMed: 9751216]

Verkhratsky A. Physiology and pathophysiology of the calcium store in the endoplasmic reticulum of neurons. Physiol Rev 2005;85:201–279. [PubMed: 15618481]

Wallner M, Hanchar HJ, Olsen RW. Ethanol enhances alpha 4 beta 3 delta and alpha 6 beta3 delta gamma-aminobutyric acid type A receptors at low concentrations known to affect humans. Proc Natl Acad Sci U S A 2003;100:15218–15223. [PubMed: 14625373]

Wang B, Rothberg BS, Brenner R. Mechanism of β_4 subunit modulation of BK channels. J Gen Physiol 2006;127:449–465. [PubMed: 16567466]

Weiger TM, Hermann A, Levitan IB. Modulation of calcium-activated potassium channels. J Comp Physiol A Neuroethol Sens Neural Behav Physiol 2002;188:79–87. [PubMed: 11919690]

Wu G, Miller KW. Ethanol enhances agonist-induced fast desensitization in nicotinic acetylcholine receptors. Biochemistry 1994;33:9085–9091. [PubMed: 8049210]

Xia XM, Zeng X, Lingle CJ. Multiple regulatory sites in large-conductance calcium-activated potassium channels. Nature 2002;418:880–884. [PubMed: 12192411]

Zeng XH, Xia XM, Lingle CJ. Divalent cation sensitivity of BK channel activation supports the existence of three distinct binding sites. J Gen Physiol 2005;125:273–286. [PubMed: 15738049]

Zhang L, Hosoi M, Fukuzawa M, Sun H, Rawlings RR, Weight FF. Distinct molecular basis for differential sensitivity of the serotonin type 3A receptor to ethanol in the absence and presence of agonist. J Biol Chem 2002;277:46256–46264. [PubMed: 12368287]
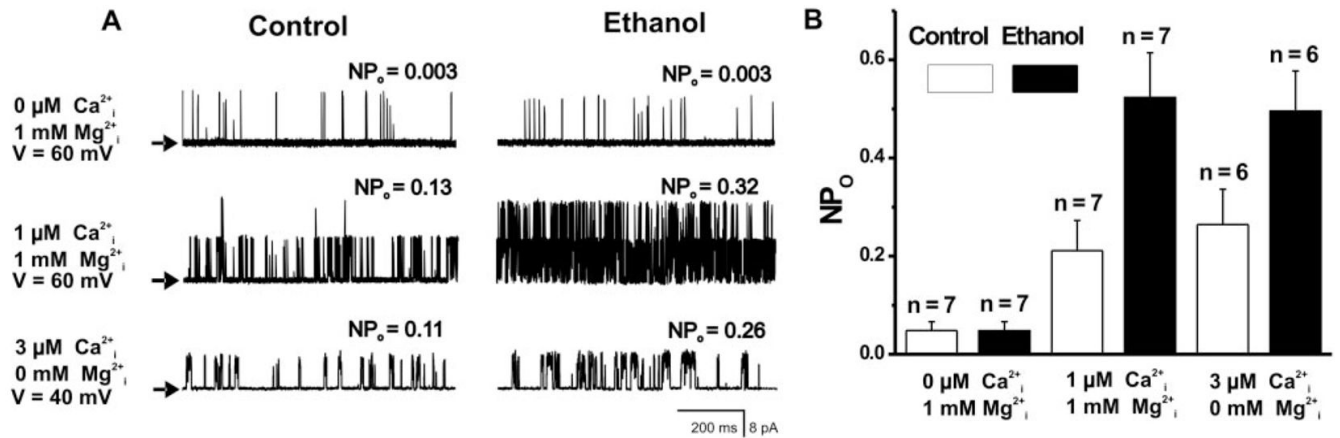
Fig. 1.
Calcium is necessary and sufficient for ethanol to modulate BK_{Ca} channel activity. A, single-channel recordings from the I/O patches with the cytosolic side of the patch exposed to 0 $Ca_i^{2+}/1\,mM\,Mg_i^{2+}$ (upper), $1\,\mu M\,Ca_i^{2+}/1\,mM\,Mg_i^{2+}$ (middle), or $0\,Ca_i^{2+}/zero\,Mg_i^{2+}$ (bottom) bath solutions in the presence (right) or absence (left) of 100 mM ethanol. Channel openings are upward deflections; arrows indicate the baseline. Averages are shown in B. NP_o was obtained from 60 s under each condition; $V = 40$ to 60 mV.
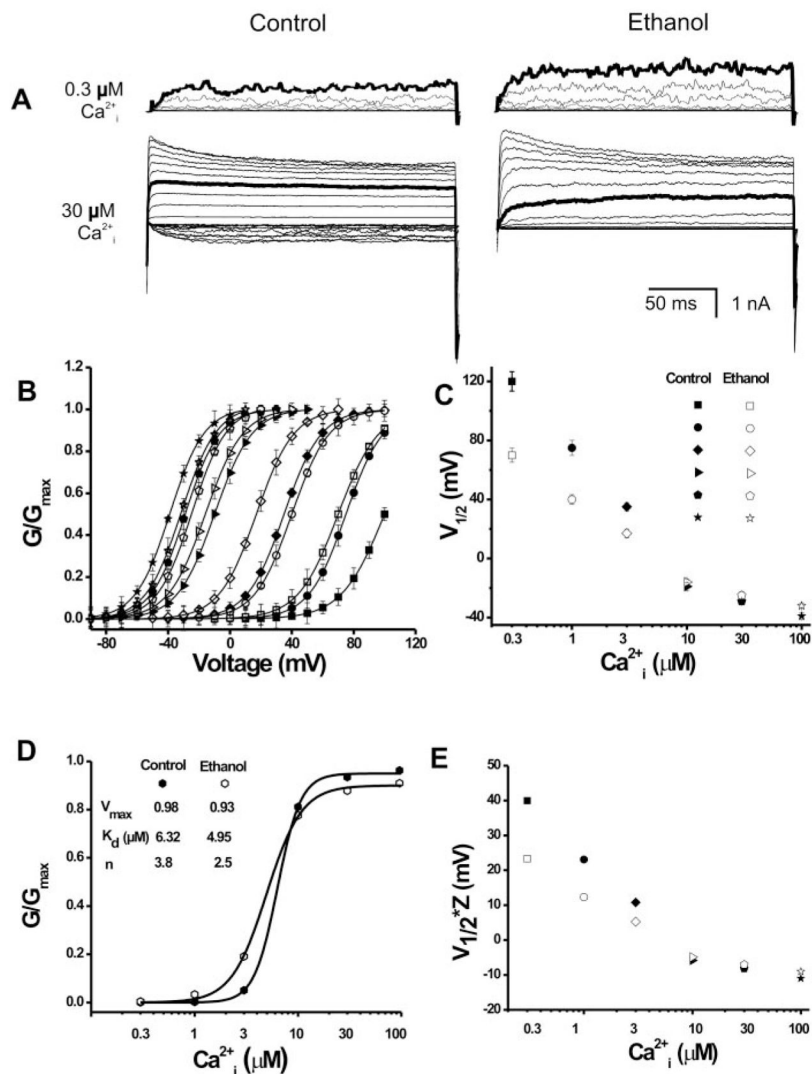
Fig. 2.

Ethanol potentiates current at submicromolar Ca_i^{2+} while inhibiting current at higher Ca_i^{2+} levels. A, macropatch recordings in 0.3 or 30 μM Ca_i^{2+} before and after 100 mM show ethanol dual action as a function of Ca_i^{2+} (highlighted by bolding a selective current trace: 100 mV at 0.3 μM and 40 mV at 30 μM). In addition, ethanol inhibition can be clearly seen from drug reduction of inward currents at 30 μM Ca^{2+}. B, whether activating or inhibiting current, ethanol causes parallel shifts in the G/G$_{max}$-V plots. C, the overall rate of decay in $V_{1/2}$ as function of Ca_i^{2+} is reduced by ethanol. D, a G/G_{max}-Ca^{2+} plot highlights ethanol biphasic action, which results in reduced E_{max}, K_d, and n for Ca^{2+} (see main text); $V = 0$ mV. E, $z \times V_{1/2}$-Ca^{2+} plots for the conditions shown in C. For B–E, filled, control; hollow symbols, ethanol. The symbol shapes in B and D match those in the $V_{1/2}$ plots shown in C and E, with each symbol corresponding to a Ca_i^{2+} concentration given in abscissa of plots in C and E.
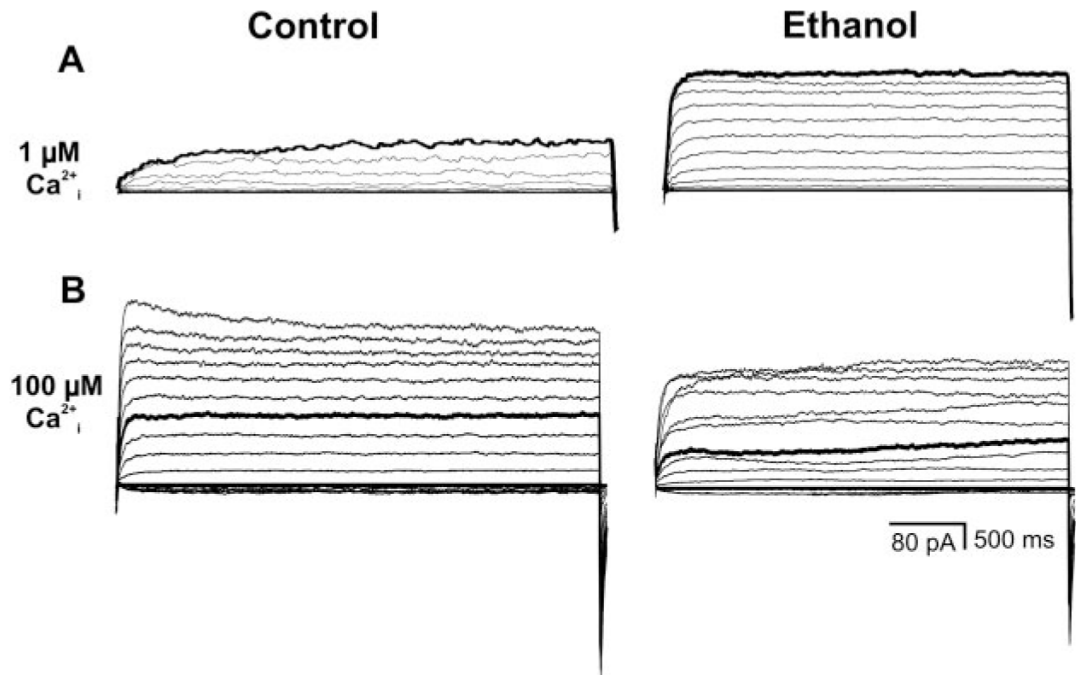
Fig. 3.
Ethanol at concentrations obtained in blood after moderate to heavy episodic drinking potentiates current at submicromolar Ca_i^{2+} while inhibiting current at higher Ca_i^{2+} levels. Current traces from the same I/O macropatch obtained in 1 μM (top) or 100 μM Ca_i^{2+} (bottom) in absence (left) or presence (right) of 50 mM ethanol show that at every potential step, the alcohol increases current at $Ca_i^{2+} < 10\,\mu$M while decreasing current at $Ca_i^{2+} > 10\,\mu$M (highlighted by bolding a selective current trace: 100 mV at 1μM and 40 mV at 100 μM free Ca_i^{2+}). Results are identical to those obtained with higher ethanol concentrations (Fig. 2). Currents were evoked and measured as described under *Materials and Methods*.
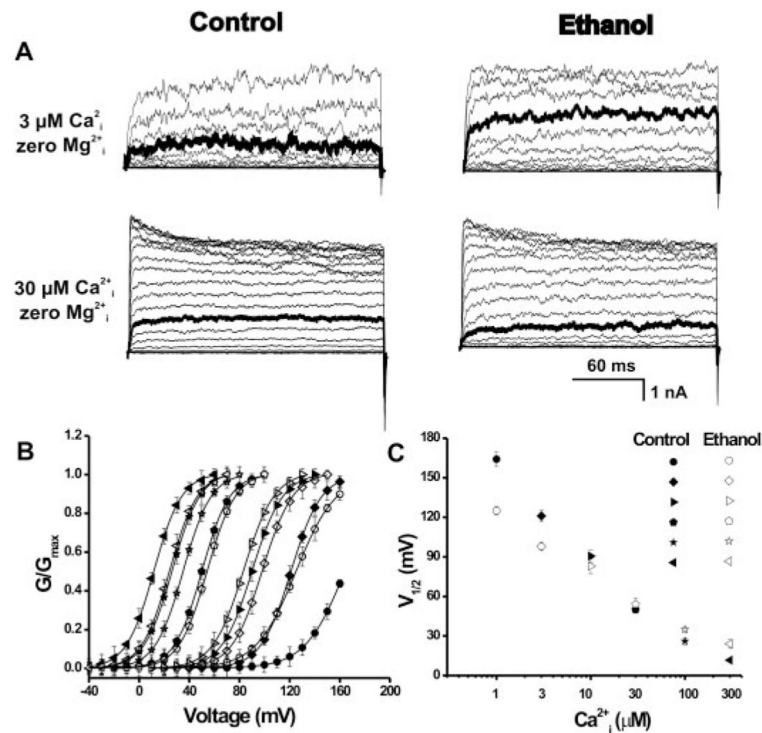
Fig. 4.

In the absence of Mg_i^{2+}, ethanol also exerts dual actions on BK_{Ca} channel currents as a function of Ca_i^{2+}. A, current traces from the same I/O macropatches obtained in 0 Mg_i^{2+} and 3 μM Ca_i^{2+} in the absence (top) and presence (bottom) of 100 mM ethanol. As found in the presence of Mg^{2+} (Fig. 2), ethanol increases current (250% of control) at 3 μM Ca_i^{2+} ($V = 130$ mV) while decreasing current (70% of control) at 30 μM Ca_i^{2+} ($V = 50$ mV). B, G/G_{max} versus $[Ca^{2+}]_i$ plots fit to Boltzmann functions. C, ethanol dual action is reflected as a reduction in the steepness of the $V_{1/2}$ versus $[Ca^{2+}]_i$ plot, as found in Mg_i^{2+} presence (Fig. 2) Currents were evoked and measured as described under *Materials and Methods*.
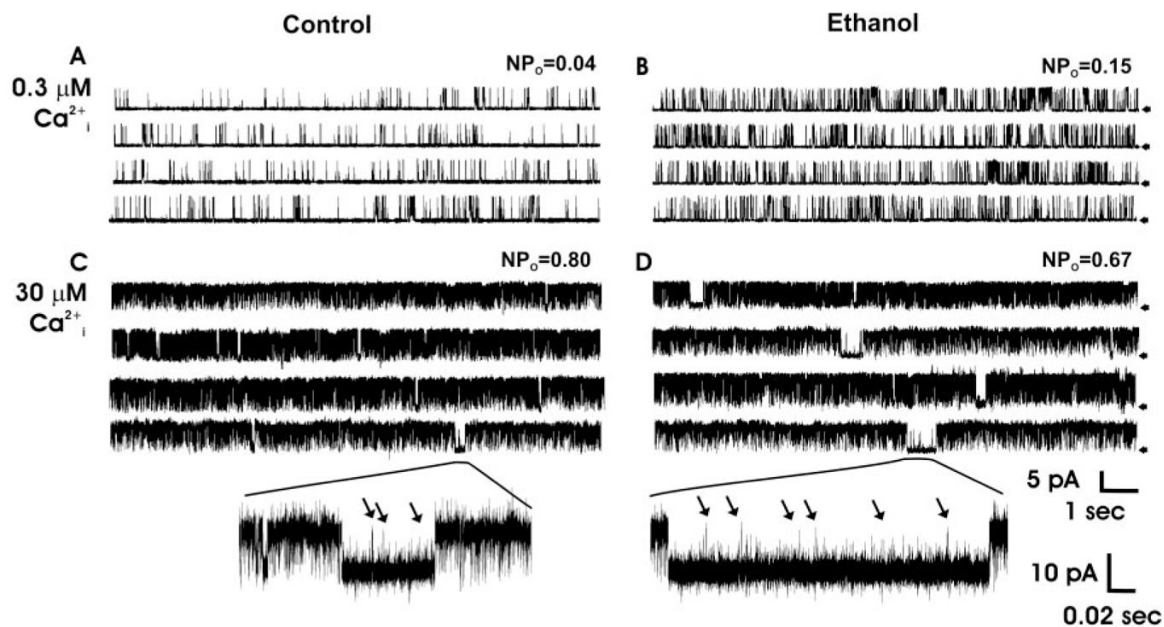
Fig. 5.
Ethanol dual actions on macroscopic current result from drug dual actions on P_o show unitary current traces from the same I/O patch obtained at 0.3 and 30 μM Ca_i^{2+}, before (A and C) and after (B and D) 100 mM ethanol exposure. Without modifying unitary current amplitude (see main text), ethanol increases P_o at Ca_i^{2+} below 10 μM (B versus A) while decreasing P_o at Ca_i^{2+} above 10 μM (D versus C). Openings are upward deflections; horizontal arrows indicate the baseline. Ca^{2+}-favors channel dwelling into ~0.5-s periods of low P_o. This "low-activity mode" (Rothberg et al., 1996) includes flickery openings (see time-expanded traces obtained from the bottom trace in C and D). Ethanol further facilitates the channel dwelling into the low-activity mode (D versus C). Data were low-pass-filtered at 7 kHz and digitized at 35 kHz. V was set to 60 mV.
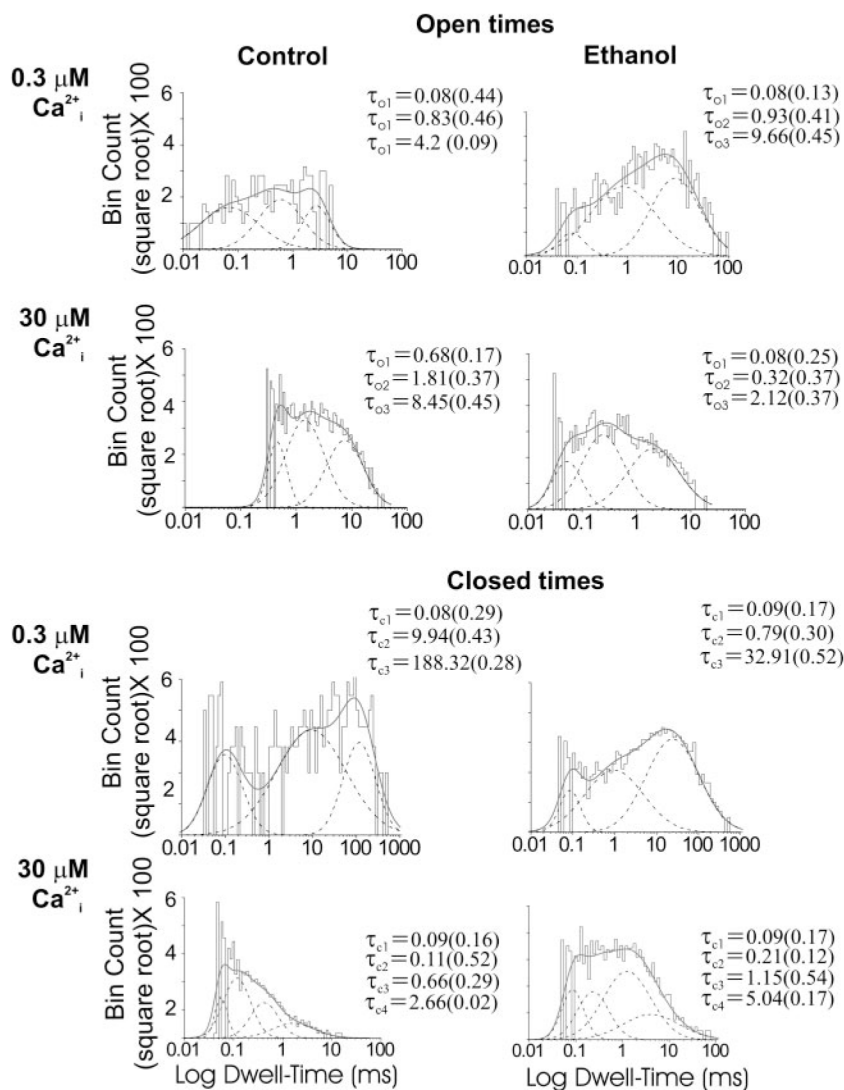
Fig. 6.
Ethanol changes channel P_o by modifying both open- and closed-time distribution. Open- and closed-time distributions in the absence (left) or presence (right) of 100 mM ethanol in 0.3 μM Ca_i^{2+} (first and third rows) and 30 μM Ca_i^{2+} (second and fourth rows). Each shows the duration of each particular component (τ, in milliseconds), and the relative contribution of each particular component to the total fit (in parentheses). The number of events was normalized before applying a Sigworth-Sine transformation, as done previously (Crowley et al., 2003), which allows a better resolution of the individual components. For a description of ethanol actions on the channel dwell times, please see main text. Dashed lines indicate the individual exponential components of the fit, and solid lines indicate the composite fit.
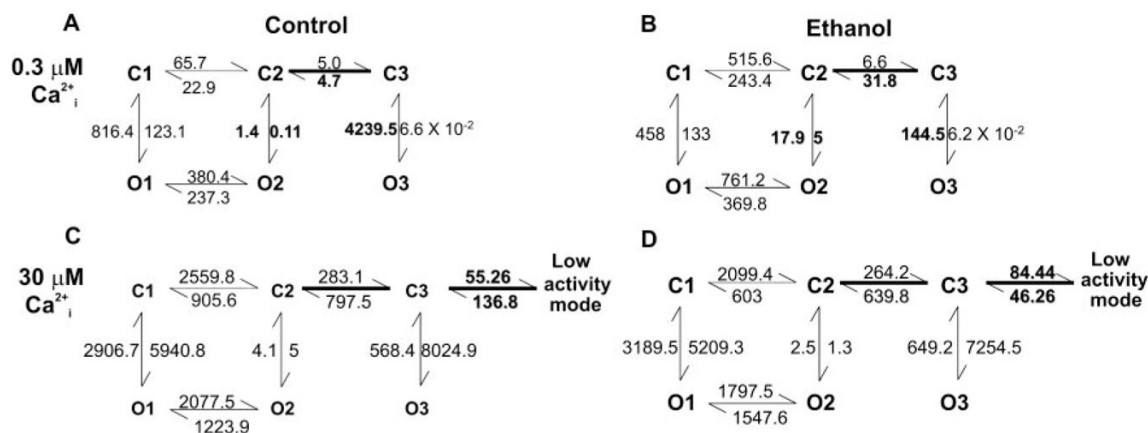
Fig. 7.
Simple, empiric kinetic models identify rate constants altered by ethanol and calcium, which explain ethanol dual actions on P_o. The figure shows the final kinetic model for each experimental condition, obtained after optimization by QuB. At high Ca_i^{2+}, channel activity could be satisfactorily modeled only by introducing an additional component corresponding to the Ca^{2+}-driven, low-activity mode (C versus A). At low Ca_i^{2+}, ethanol prevents channel entry into long closed states by increasing the C3→C2 transition and decreasing O3→C3. In addition, ethanol stabilizes openings within the normal-activity mode by shifting the O2↔C2 equilibrium toward O2 (B versus A). These actions explain ethanol's increase in P_o (Fig. 3). Indeed, P_o values calculated from the model rate constants (control, 0.05; ethanol, 0.2) match those obtained from all-points amplitude histograms (control, 0.04; ethanol, 0.16). At high Ca^{2+}, ethanol mildly diminishes the C3→C2 transition and drastically shifts the C3↔ low activity mode equilibrium toward the latter (×5 times) (D versus C), favoring channel dwelling within the low-activity mode. These actions explain ethanol's decrease in P_o (Fig. 3). Indeed, P_o values calculated from the rate constants (control, 0.79; ethanol, 0.7) also match those obtained from all-points amplitude histograms (control, 0.8; ethanol, 0.67). Data for kinetic modeling were obtained from ≥5 min of continuous recording, low-pass-filtered at 10 and digitized at 50 kHz. V was set to 60 mV. C1–C3, closed states; O1–O3, open states.
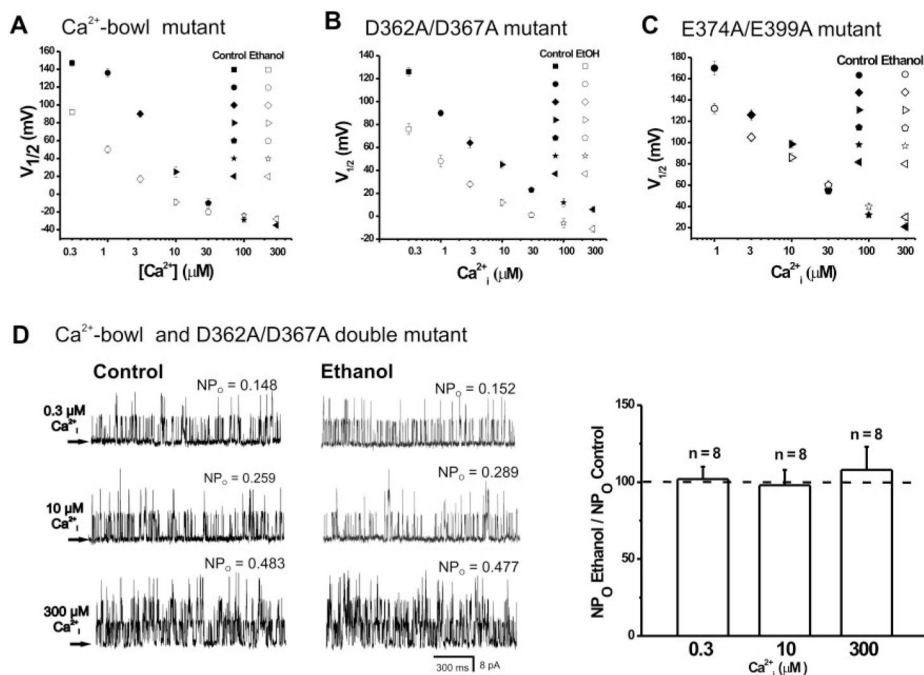
Fig. 8.
The two high-affinity Ca^{2+}-recognition sites in slo1 are sufficient, yet none necessary, for ethanol to modulate channel function. $V_{1/2}$- Ca_i^{2+} plots demonstrate that mutations in the Ca^{2+}-bowl (5D5N) ($n = 8$) (A) or the RCK1 low-affinity Ca^{2+}-recognition site (E374A/E300A) ($n = 9$) (C) fail to eliminate ethanol dual action (evident by a drug-decrease in slope; compare Figure 2C). In contrast, mutations in the RCK1 high-affinity site (D362A/D367A) abolish ethanol inhibition of current ($n = 9$) (evident from the similar $V_{1/2}$- Ca_i^{2+} plot slopes in control and ethanol) (B). In all these constructs, ethanol potentiation of current at low Ca^{2+} is observed (A–C). In contrast, this ethanol action is lost when the 5D5N and the D362A/D367A mutations are combined (D). Left, single-channel recordings in absence and presence of ethanol at 0.3, 10, and 300 μ M Ca_i^{2+}; $V_m = 80$ mV; right, average responses.
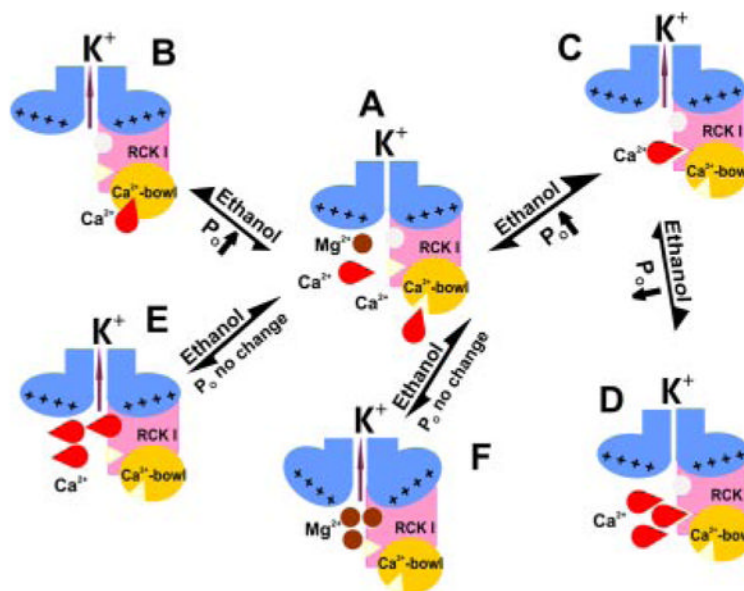
Fig. 9.
Diagram illustrating our interpretation of ethanol modulation of BK_{Ca} channel activity. A lateral view (normal to the bilayer surface) of the BK_{Ca} channel is shown as a dimmer of slo1 subunits, with their relevant domains shown only in one monomer: the "core" (conducting and voltage-sensing machinery) is shown in blue; the RCKI domain is in pink; the Ca^{2+} bowl is in yellow. At lower Ca_i^{2+}, the equilibria from nonconducting (A) to conducting states due to Ca^{2+}-sensing by the Ca^{2+}-bowl (B) or by the RCK1 high-affinity site (C) are shifted toward the conducting states (see relative sizes of arrow heads) by ethanol, rendering increased P_o.

The RCK1 high-affinity site sensing of higher $[Ca_i^{2+}]$ makes the channel dwell in a low-activity mode (D), this dwelling being favored by ethanol, diminishing overall P_o. In contrast, ethanol does not modify gating involving the RCK1 low-affinity site and determined by micromolar-millimolar divalent, whether Ca^{2+} (E) or Mg^{2+} (F). Ethanol does not affect gating involving the voltage sensor (moving upward from A to F). Brown arrows, outward K^+ flow; plus symbols, voltage sensor; circular "pockets," RCK1 low-affinity Ca^{2+} site; triangular notch, high-affinity Ca^2 sites in RCK1 or "bowl"; brown circles, Mg^{2+}; red drops, Ca^{2+}.